



Self-assembly of achiral monomer into left-handed helical polyanthracene nanofibers

Bing Han^{1,†}, Fangping Shen^{2,†}, Hong Su¹, Xin Zhang³, Yang Shen^{3,*}, and Ting Zhang^{2,*}

¹Department of Orthodontics, School and Hospital of Stomatology, Peking University, Beijing 100081, China

²Suzhou Institute of Nano-Tech and Nano-Bionics, Chinese Academy of Sciences, Suzhou 215123, China

³School of Materials Science and Engineering, State Key Lab of New Ceramics and Fine Processing, Tsinghua University, Beijing 100084, China

ABSTRACT

Bionic control over the assembly of achiral molecules into chiral supramolecular architectures is challenging, and typically relies on preexisting templates. We demonstrated that anthracene monomers could self-assemble into polyanthracene (PA) nanofibers with well-defined left-handed helical nanoarchitectures under well-controlled conditions. The spontaneous formation of supramolecular helices might be ascribed to the steric constraints imposed by dehydrocyclization carried out at the 4,8 sites of the benzene ring of the anthracene monomer. Furthermore, high quality, few-layer graphene, derived from the chiral helical PA nanofibers, provided promising prospects and new ideas for functional materials synthesis and chirality amplification.

Keywords: Self Assembly, Achiral, Helical, Nanofibers, Polyanthracene.

1. INTRODUCTION

As a fundamental attribute of nature, chirality is observed in most of the basic building blocks of life, such as DNA and proteins.⁽¹⁾ Biomimetic chiral materials use chirality as a key structural factor, and have displayed a series of complicated functions in materials science, and as chemical and biological sensors,⁽²⁾ pharmaceuticals, and for enantioselective separation.^(3,4) Generally, chirality of a system involves intrinsically chiral molecules and chiral assemblies. With asymmetric carbon atoms or conformational asymmetry, chiral molecules form chiral assemblies by non-covalent interactions. To simulate this principle, a variety of templates have been introduced to change the intrinsic assembly modes of achiral molecules to achieve highly ordered chiral nanoarchitectures with a wide range of applications.^(5,6) However, template-dependent chiral assembly significantly restricts the expression of the inherent chirality and breaking of symmetry. Self-assembly,

making use of molecular, rather than atomic, units, offers a promising bottom-up approach to the construction of functional materials in a template-free fashion.^(7,8) However, it remains a great challenge to precisely control the self-assembly of simple achiral molecules into elaborate chiral supramolecular architectures.

Polyanthracene (PA), one of the most important intrinsic conducting polymers, has exhibited excellent optical and electronic properties, such as high charge carrier mobility, superradiance and fluorescence anisotropy.⁽⁹⁾ The structure-property relationship of PA has been well established. Their optical and electronic properties depend not only on the molecular packing, structural defects and material purity, but also on the dimension.⁽¹⁰⁾ It is thus of practical importance to manipulate the molecular organization and spatial orientation of these molecular systems for applications requiring optoelectronic nanodevices. PA could be fabricated by anthracene molecules using electrochemical polymerization,⁽¹¹⁾ by a chemical route,^(12,13) and through the surface catalysis of Au(111).⁽¹⁴⁾ With chiral dopants of properly folded DNA or polypeptide chains

*Authors to whom correspondence should be addressed.

Emails: tzhang2009@sinano.ac.cn, shyang_mse@tsinghua.edu.cn

[†]These authors contributed equally to this work.

as templates, the helical conformation of several conducting polymers has been obtained by ionic interaction.^(15, 16) However, PA nanofibers with chiral supramolecular architectures have not been reported. The self-assembly synthesis of pure chiral helical conducting polymers, taking advantage of both conducting polymers and chiral nanostructures, still remains a scientific obstacle.

In this communication, we observed that under well-controlled conditions, anthracene monomers could self-assemble into arrays of left-handed chiral helical PA nanofibers in a template-free manner. The spontaneous formation of chiral helices may be initiated by the steric constraints imposed by dehydrocyclization carried out at the 4, 8 sites of the benzene ring of the anthracene monomer. The PA nanofibers were also used in organic protocols leading to few-layer graphene. This study could

provide new insights into the regulation of chirality amplification, which would extend our ability to control the self-assembly of achiral monomers and develop novel functional materials.

2. EXPERIMENTAL DETAILS

PA was synthesized through oxidative coupling polymerization from simple anthracene monomers. Anhydrous CH_3NO_2 and CHCl_3 were dried in a 4 Å molecular sieve, followed by distillation. All the glass instruments were dried at 120 °C for 12 h. 25 ml of pre-processed anhydrous CH_3NO_2 were placed in a 250 ml three-necked flask (which had received full replacement of N_2). Anhydrous FeCl_3 (4 g) was then added under the protection of N_2 and strong stirring was carried out until the FeCl_3 completely

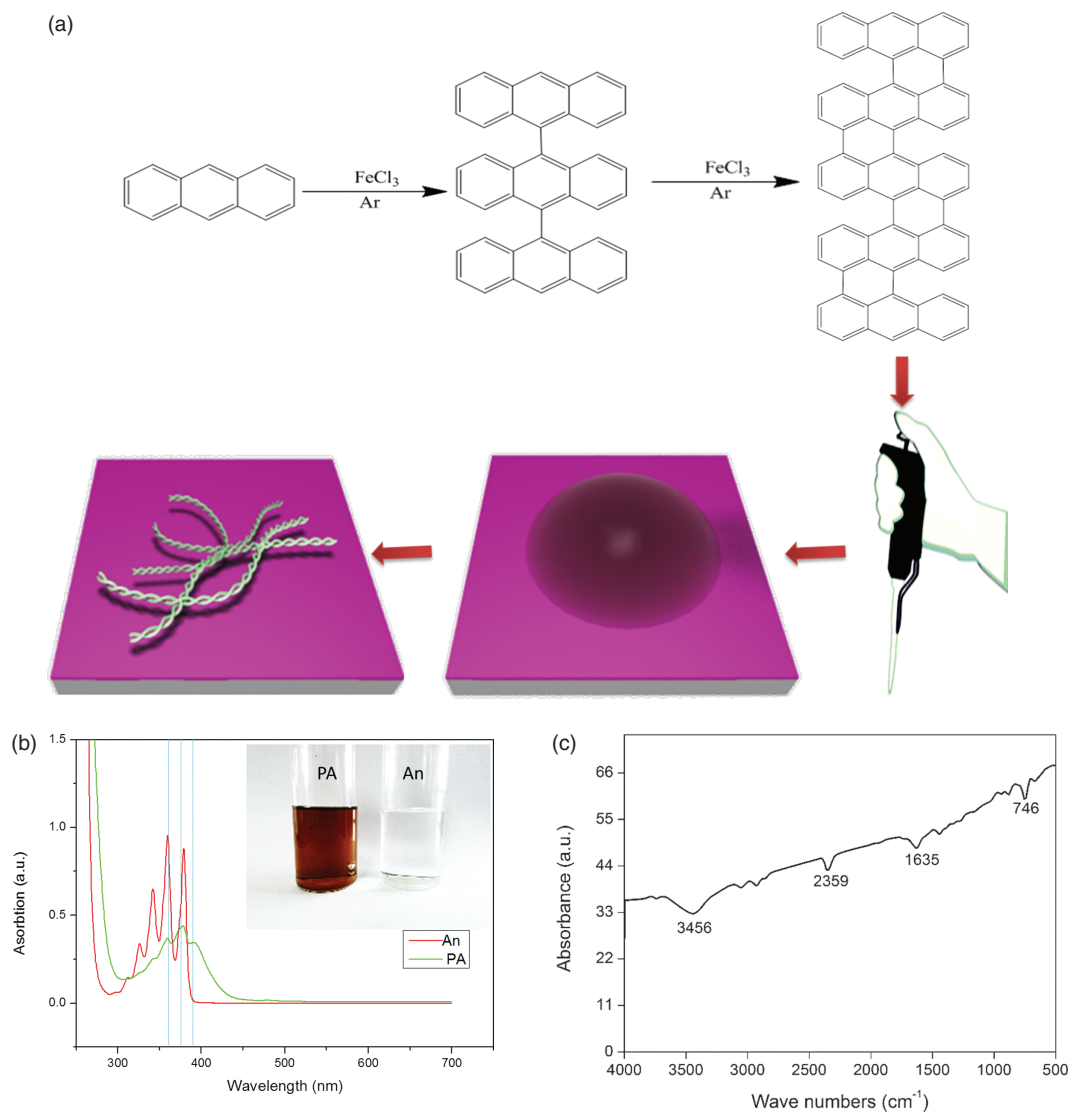


Fig. 1. (a) Schematic illustration of the process of anthracene monomer self-assembly into arrays of left-hand chiral helical PA nanofibers in a template-free manner, (b) UV spectra of anthracene (An) and PA. The inset shows the solution of An (transparent and colorless) and PA (brown), (c) The FT-IR spectrum of PA.

dissolved. Then 0.5 g of simple anthracene was added into a 100 ml stand-up flask (which had received full replacement of N_2), followed by injection of 50 ml Anhydrous $CHCl_3$. After the majority of the anthracene had dissolved, the anthracene/ $CHCl_3$ solution was transferred into the three-necked flask with strong stirring. The reaction was held for 48 h at RT (room temperature) until the solution turned viscous and dark brown. The fully reacted mixture was suction filtered and washed with acetone and methylbenzene, respectively, three times, to remove the PA with a low degree of polymerization. The pre-purified PA was then transferred into a cylindrical filter paper and the backflow was carried out with methyl alcohol in a soxhlet extraction system until the methyl alcohol in the siphon turned colorless. The final purified PA was dried under a vacuum.

PA nanofibers with left-handed helical architecture were synthesized through a self-assembly process induced by solvent evaporation. A drop of PA/ $CHCl_3$ solution was spread out on a polished silicon wafer, and then exposed to air at room temperature till the $CHCl_3$ completely evaporated. The final silicon wafer was characterized using SEM.

Few-layer graphene were synthesized from PA nanofibers. Dried PA nanofibers (0.5 g) were calcined at 400 °C under an Ar atmosphere for 4 h. The calcined black powders were then ultrasonically dispersed in $CHCl_3$. The supernatant liquid was collected and deposited on Si substrates for the TEM characterization.

3. RESULTS AND DISCUSSION

To controllably synthesize PA nanostructures, high quality PA was first prepared using strong Lewis acidoxidative

polymerization of anthracene monomers (Fig. 1(a)). The polymerization behavior was studied in aqueous chloroform solution using UV-visualization (Fig. 1(b)). The spectrum of anthracene in aqueous solution exhibited a strong absorbance between 300 and 400 nm, with pronounced vibronic structures producing peaks at 326, 342, 359 and 379 nm because of the $\pi-\pi^*$ transition. A red shift of absorption bands of approximately 80 nm red was observed in PA compared with the anthracene monomer. This shift could be assigned to the increase in the magnitude of the conjugation system and the decrease of the band gap values between π and π^* after polymerization.⁽¹¹⁾ Furthermore, the characteristic broad bands in Fourier transform infrared (FT-IR) spectroscopy measurement (Fig. 1(c)) of around 746 cm^{-1} , 1635 cm^{-1} , 2359 cm^{-1} and 3456 cm^{-1} , clearly showed that PA was successfully achieved.

Chiral, helical nanostructure was then observed after drop-casting a PA/ $CHCl_3$ solution on a silicon substrate at room temperature. The evidence for the formation of chiral nanofibers was provided by scanning electron microscope (SEM) (Fig. 2). Typical homogeneous, chiral, helical nanofibers, with lengths up to several micrometers and widths of about twenty nanometers, were achieved using 0.02 mM of PA/ $CHCl_3$ solution (Figs. 2(b) and (e)). The widths of the nanofibers could be adjusted by altering the concentration of the polymer solutions. When the concentration of the polymer solution was lower than 0.02 mM, heterogeneous chiral helices with smaller diameters and many spherical beads were fabricated (Figs. 2(a) and (d)). A higher concentration of 0.04 mM yielded nanofibers with larger widths accompanied by increased

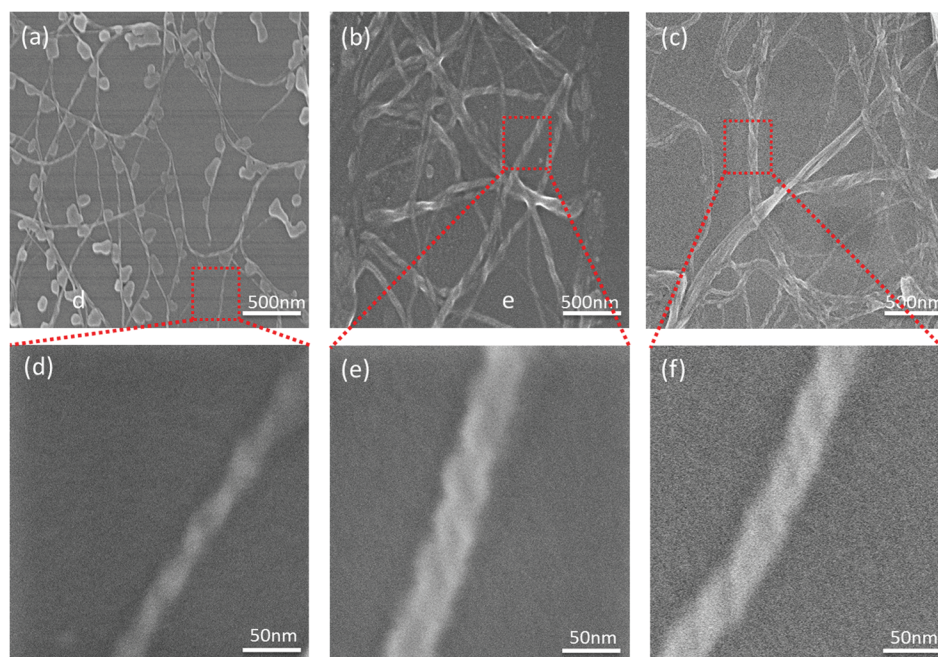


Fig. 2. SEM images of PA nanofibers. PA nanofibers deposited on the silicon substrate at a concentration of 0.01 mM (a), (d), 0.02 mM (b), (e) and 0.04 mM (c), (f). The lower images are enlargements of specific regions of the upper images.

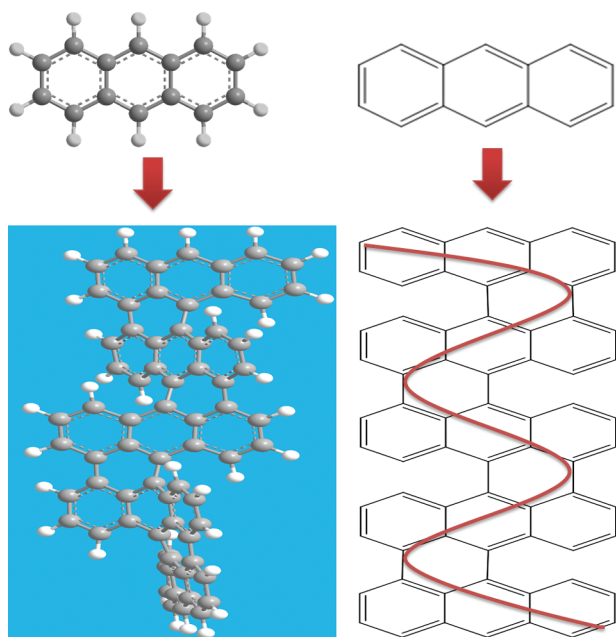


Fig. 3. Schematic illustration of the formation of supramolecular PA helices because of the steric constraints imposed by dehydrocyclization carried out at the 4, 8 sites of the benzene ring of the anthracene monomer.

heterogeneity (Figs. 2(c) and (f)). However, under a saturated vapor environment, no nanofibers formed on the substrate after solvent evaporation. It should be noted that all these fabricated nanofibers had a chiral, left-handed helical architecture. Chirality was not only expressed by single helical nanofibers, but also by the supramolecular structures: two or more the single helical fibers intertwined with each other to form a superhelix. To the best of our knowledge, this is the first experimental observation of helically chiral structures in PA.

PA has shown great potential in electrical, optical, and chemical active materials and devices.^(17,18) Herein, we report a one-step growth of left-handed helical PA nanofibers. The mechanisms involved in the superstructure formation might be interpreted in terms of molecular

self-assembly of anthracene (Fig. 3). Anthracene is a polycyclic aromatic hydrocarbon composed of three linearly fused benzene rings. In the common polymerization system, coupling occurs at the 9, 10 sites on the benzene ring of anthracene to fabricate symmetric PA.^(11,12) However, it is important to note that the catalyst used in this study was FeCl₃, which can catalyze coupling polymerization as well as dehydrocyclization. In this sense, we hypothesized that the dehydrocyclization might be carried out at the 4, 8 sites of the benzene ring. Once dehydrocyclization happened, the steric hindrance between the rigid linear planar structures of the anthracene molecules was strengthened and further dehydrocyclization at the same side would be prevented or at least become difficult. Thus, the stereoselectivity of the whole PA chain favored the self-assembly of anthracene into cylindrical micelles, in which the molecules are aligned perpendicularly to the cylinder axis.⁽¹⁹⁾ In addition, the rod segments would stack on top of each other with mutual rotation in the same direction to avoid steric hindrance between the bulky dendritic wedges. Consequently, this stacking of the aromatic rod segments would lead to helical objects, comprising hydrophobic aromatic cores, surrounded by hydrophilic dendritic segments that are exposed to the aqueous environment. Specifically, the helical single strand PA fibers constructed through the self-assembly of anthracene monomers was believed to have arisen from steric constraints imposed by dehydrocyclization. The observed supramolecular handedness may be attributed to the strong π - π stacking and van der Waals interactions among multiple-strand nanofibers.

To further explore the application of PA nanofibers with helix, chiral structures, they were used in organic synthetic protocols leading to graphene type molecules. The lamellar graphene (tens of nm in size) were achieved after annealing of PA nanofibers at 400 °C in Ar. The edges of the obtained graphene were generally curled, which might reflect the chiral structure of the PA nanofibers (Figs. 4(a) and (b)). The Raman spectrum was used to reveal the structural characteristic of the as achieved graphene. The main features in the Raman spectra of

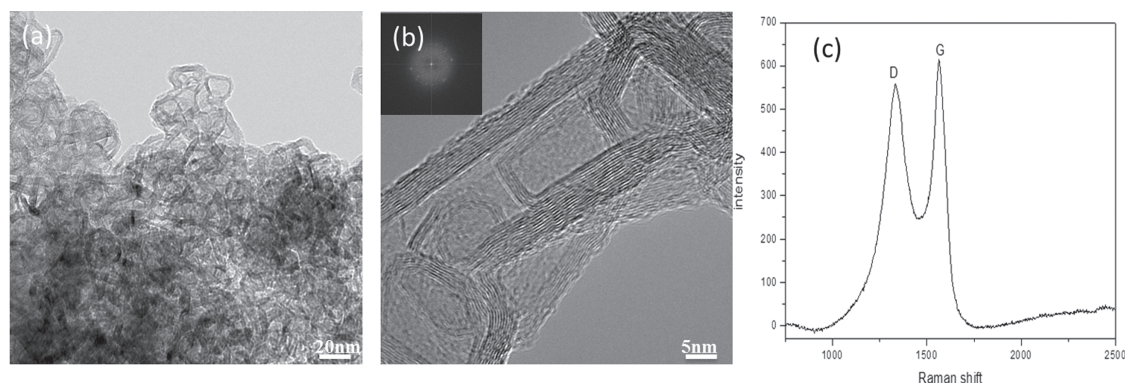


Fig. 4. TEM images (a), (b) and Raman spectra (c) of PA-derived few-layer graphene.

graphene are the so-called G and D peaks.⁽²⁰⁾ The G peak is due to the bond stretching of all pairs of sp^2 atoms in both rings and chains. The D peak is due to the breathing modes of sp^2 atoms in rings. Intensity ratio of D and G peaks I_D/I_G indicates the degree of disordered structures in graphene. In this work, G peak at 1584 cm^{-1} and D peak at 1332 cm^{-1} represent graphitic and disordered structures of graphene, respectively (Fig. 4(c)). The high strength ratio of I_D/I_G (close to 1) suggested that high quality graphene was fabricated.⁽²¹⁾ This result may provide a strategy to design graphene-like structures made by two-dimensional polymerization of simple monomers.

4. CONCLUSION

We have achieved left-handed, chiral, helical PA nanofibers using a simple solvent evaporation method. The growth of nanofibers might be attributed to self-assembly of anthracene monomers initiated by the steric constraints imposed by dehydrocyclization carried out at the 4, 8 sites of the benzene ring. Few-layer graphene, derived from the chiral helical PA nanofibers, further demonstrated that the impact of this work would go far beyond a simple proof-of-concept of self-assembly of achiral monomer into chiral helical nanostructures. Our strategy may provide new ideas to design chiral, helical conducting nanomaterials for multiple practical applications.

Acknowledgments: This work was supported by grants from the National Basic Research Program of China (2015CB351900, 2012CB933900), the National High Technology Research and Development Program of China (2012BAI07B00), the Key International S&T Cooperation Project (2011DFA32190), the National Natural Science Foundation of China (91123034, 61574163, 81171000, 51302005), the Beijing Natural Science Foundation (7144256, 7144257), the Doctoral Scientific Fund Project of the Ministry of Education of China (20130001120112) and the Beijing Nova Program (Z14111000180000).

References and Notes

1. A. Kuzyk, R. Schreiber, Z. Fan, G. Pardatscher, E. Roller, A. Högele, F. C. Simmel, A. O. Govorov, and T. Liedl; DNA-based self-assembly of chiral plasmonic nanostructures with tailored optical response; *Nature* 483, 311 (2012).
2. S. Kang, I. Cha, J. G. Han, and C. Song; Electroactive polymer sensors for chiral amines based on optically active 1,1'-binaphthyls; *Mater. Express* 3, 119 (2013).
3. J. Huang, V. M. Egan, H. Guo, J. Y. Yoon, A. L. Briseno, I. E. Rauda, R. L. Garrell, C. M. Knobler, F. Zhou, and R. B. Kaner; Enantioselective discrimination of D- and L-phenylalanine by chiral polyaniline thin films; *Adv. Mater.* 15, 1158 (2003).
4. S. Fireman-Shoresh, I. Popov, D. Avnir, and S. Marx; Enantioselective, chirally templated sol-gel thin films; *J. Am. Chem. Soc.* 127, 2650 (2005).
5. Y. Yin, Y. Lu, B. Gates, and Y. Xia; Template-assisted self-assembly?: A practical route to complex aggregates of monodispersed colloids with well-defined sizes, shapes, and structures; *J. Am. Chem. Soc.* 123, 8718 (2001).
6. Y. Xia, Y. Yin, Y. Lu, and J. McLellan; Template-assisted self-assembly of spherical colloids into complex and controllable structure; *Adv. Funct. Mater.* 13, 907 (2003).
7. C. C. Lee, C. Grenier, E. W. Meijer, and A. P. Schenning; Preparation and characterization of helical self-assembled nanofibers; *Chem. Soc. Rev.* 38, 671 (2009).
8. R. P. Sugavaneshwar, T. Nagao, and K. K. Nanda; Fabrication of highly dense nanoholes by self-assembled gallium droplet on silicon surface; *Mater. Express* 2, 245 (2012).
9. N. K. Desai, G. B. Kolekar, and S. R. Patil; Off-on fluorescent polyanthracene for recognition of ferric and fluoride ions in aqueous acidic media: Application in pharmaceutical and environmental analysis; *New J. Chem.* 38, 4394 (2014).
10. I. O. Shklyarevskiy, P. Jonkheijm, P. C. Christianen, A. P. Schenning, A. Del Guerzo, J. P. Desvergne, E. W. Meijer, and J. C. Maan; Magnetic alignment of self-assembled anthracene organogel fibers; *Langmuir* 21, 2108 (2005).
11. B. Fan, L. Qu, and G. Shi; Electrochemical polymerization of anthracene in boron trifluoride diethyl etherate; *J. Electroanal. Chem.* 575, 287 (2005).
12. I. Schopov and C. Jossifov; Synthesis and properties of 1,5- and 1,8-dichloro-substituted poly(9,10-dihydroanthracene-9,10-diylidene)s; *Polymer* 23, 613 (1982).
13. I. Schopov and C. Jossifov; Synthesis and properties of poly(9,10-anthracene diylidene)s; *Polymer* 19, 1449 (1978).
14. J. Cai, P. Ruffieux, R. Jaafar, M. Bieri, T. Braun, S. Blankenburg, M. Muoth, A. P. Seitsonen, M. Saleh, X. Feng, K. Müllen, and R. Fasel; Atomically precise bottom-up fabrication of graphene nanoribbons; *Nature* 466, 470 (2010).
15. Y. Yan, Z. Yu, Y. Huang, W. Yuan, and Z. Wei; Helical polyaniline nanofibers induced by chiral dopants by a polymerization process; *Adv. Mater.* 19, 3353 (2007).
16. J. Huang, S. Virji, B. H. Weiller, and R. B. Kaner; Polyaniline nanofibers: Facile synthesis and chemical sensors; *J. Am. Chem. Soc.* 125, 314 (2003).
17. K. Tanemura, T. Suzuki, and T. Horaguchi; Synthesis of sulfonated polynaphthalene, polyanthracene, and polypyrene as strong solid acids via oxidative coupling polymerization; *J. Appl. Polym. Sci.* 127, 4524 (2013).
18. A. L. Briseno, J. Aizenberg, Y. J. Han, R. A. Penkala, H. Moon, A. J. Lovinger, C. Kloc, and Z. Bao; Patterned growth of large oriented organic semiconductor single crystals on self-assembled monolayer templates; *J. Am. Chem. Soc.* 127, 12164 (2005).
19. Y. Takaguchi, T. Tajima, Y. Yanagimoto, S. Tsuboi, K. Ohta, J. Motoyoshiya, and H. Aoyama; Self-assembly and regioselective photodimerization of anthracene having a dendritic substituent; *Am. Chem. Soc.* 5, 1677 (2003).
20. A. C. Ferrari; Raman spectroscopy of graphene and graphite: Disorder, electron-phonon coupling, doping and nonadiabatic effects; *Solid. State. Commun.* 143, 47 (2007).
21. J. Kim, K. S. Choi, Y. Kim, K. T. Lim, H. Seonwoo, Y. Park, D. H. Kim, P. H. Choung, C. S. Cho, S. Y. Kim, Y. H. Choung, and J. H. Chung; Bioactive effects of graphene oxide cell culture substratum on structure and function of human adipose-derived stem cells; *J. Biomed. Mater. Res. A.* 101, 3520 (2013).

Received: 13 May 2015. Revised/Accepted: 17 August 2015.